



Research article

Sono-anatomy of the middle cervical sympathetic ganglion verified with pathology

Yu-Tao Lei^{a,1}, Yun-Xia Hao^{b,1}, Zhen Yang^b, Zhuo-Hua Lin^b, Wen Qin^c, Jun-Hao Yan^d, Yang Sun^b, Li-Gang Cui^{b,*}, Ying Fu^b^a Department of General Surgery, Peking University Third Hospital, Beijing, China^b Department of Ultrasound, Peking University Third Hospital, Beijing, China^c Department of Ultrasound, Xiangyang Central Hospital, Affiliated Hospital of Hubei University of Arts and Science, Xiangyang City, Hubei Province, China^d Department of Anatomy and Embryology, School of Basic Medical Sciences, Peking University, Beijing, China

ARTICLE INFO

Keywords:

Cadaver
Ganglia
Sympathetic
Pathology
Ultrasonography

ABSTRACT

Objectives: Cervical discomfort and other symptoms may be attributable to the middle cervical sympathetic ganglion. The aim of this study was to explore the sonographic features of this ganglion in anatomical specimens and cadavers and evaluate the feasibility of its visualization using high-resolution ultrasonography.

Methods: We examined three cervical sympathetic-ganglion specimens and two fresh cadavers using high-resolution ultrasound to explore the sonographic features of this ganglion. Basic imaging characteristics examined included the shape, echo intensity, and location of the ganglion. Core-needle biopsy was performed to examine the suspected middle cervical sympathetic ganglion in the two fresh cadavers and verify the accuracy of the sonographic identification via pathological examination.

Results: The middle cervical sympathetic ganglion appeared on high-resolution ultrasonography as an oval-shaped hypoechoic structure, with at least one continuous hypoechoic line connected to each ending in the anatomical specimens and fresh cadavers, and it was distinctly different from the adjacent lymph nodes.

Discussion: Based on an adequate understanding of both its location and sonographic features, the direct visualization of the middle cervical sympathetic ganglion using high-resolution ultrasonography is feasible.

1. Introduction

Since the first description of stellate ganglion block (SGB) in the 1920s [1], this procedure has been performed to treat various clinical symptoms, such as hallucinatory pain, facial pain, and vascular headache [2]. Traditional approaches for this ganglion block comprise palpation and radiography-guided methods. However, the injection path is adjacent to several critical structures, such as the trachea, esophagus, thyroid, inferior thyroid arteries, recurrent laryngeal nerve, phrenic nerve, and brachial plexus. Newly emerging

* Corresponding author.

E-mail address: cuiligang_bysy@126.com (L.-G. Cui).

¹ Yu-Tao Lei and Yun-Xia Hao contributed equally to this work.

high-resolution ultrasonography (HRUS) is significantly better than radiographic or palpation guidance at identifying soft tissues and the real-time monitoring of the needle tip, thus greatly reducing iatrogenic complications [3]. Hence, HRUS has gained increasing popularity for SGB guidance since 1995 [4]. However, certain challenges persist. In SGB, a local anesthetic is injected to achieve a blocking effect via diffuse infiltration surrounding the cervical sympathetic ganglia (CSG) and cervical sympathetic trunk. In addition, the efficacy of SGB is well established; however, the rates of non-significant improvement and short-term symptom recurrence remain as high as 33–66 % [5]. A possible cause of these procedure failures is anatomical variation in the CSG. The actual position of these structures is not directly visualized during current SGB procedures. Therefore, the efficacy of SGB may be improved if the precise location of the CSG is identified intraoperatively and the local anesthetic injection is targeted more accurately instead of being based on the estimated CSG location.

In addition, reports of injury to the cervical sympathetic trunk and CSG have increased with the widespread use of minimally invasive neck surgery, particularly neck lymph node biopsy and the ultrasonography (US)-guided ablation of thyroid and parathyroid nodules [6–9]. Such injuries may lead to persistent Horner syndrome, characterized by ipsilateral miosis, ptosis, and anhidrosis [10].

Therefore, identifying and localizing the CSG accurately via HRUS could allow a targeted CSG block, maximize its efficacy, and minimize procedure-related injuries during US-guided neck interventions and surgeries.

The cervical sympathetic chain comprises two to four ganglia: the superior, middle, and inferior cervical/cervicothoracic ganglia. The superior CSG lies anteriorly to the longus capitis muscle and is located at the level of C2, C3, and rarely C4. The middle CSG (mCSG) is typically located on the longus colli muscle at the level of C5–7. The inferior CSG and first thoracic ganglia are combined and named the stellate ganglion, located anteriorly to the C7 transverse process or T1 rib. Limited studies have reported the imaging characteristics of the CSG. Lee et al. [11] visualized 73 % of the superior CSG using 3T magnetic resonance imaging (MRI). Chaudhry et al. [12] demonstrated that the stellate ganglia could be precisely characterized on pre-contrast three-dimensional constructive interference in steady state MRI. These two ganglia are difficult to detect using HRUS owing to the limited acoustic window, restricted by the bones and lungs. Shin et al. [13] studied the mCSG of 52 patients using US and described its imaging appearance as a thin, bulbous, hypoechoic structure connected to at least two linear structures. However, to the best of our knowledge, no cadaveric or pathological study has confirmed this finding. Thus, further research is required to verify the anatomical and ultrasonographic imaging features of the mCSG and establish the value of such information for cervical sympathetic block and interventional procedures involving the neck.

The aim of this study was to evaluate the feasibility of directly visualizing the mCSG using HRUS in specimens and cadavers, examine the scanning skills required, and investigate the anatomical and ultrasonographic imaging features of the mCSG. The purpose was to provide evidence for a more precise SGB and the protection of this structure during minimally invasive neck surgery.

2. Results

The CSG in the three dissected specimens were clearly identified using HRUS, appearing as hypoechoic nodules with both extremities connected to the linear hypoechoic cervical sympathetic trunk (Fig. 1A and B).

The necks of the cadavers were examined bilaterally using US. They had similar sonographic features to those of the three dissected specimens. The anatomical structures adjacent to the mCSG were identified in the first cadaver (male Y) by an anatomical technician. Core-needle biopsy was performed to examine both mCSG.

All the cadaveric sampling results were recorded in Table 1.

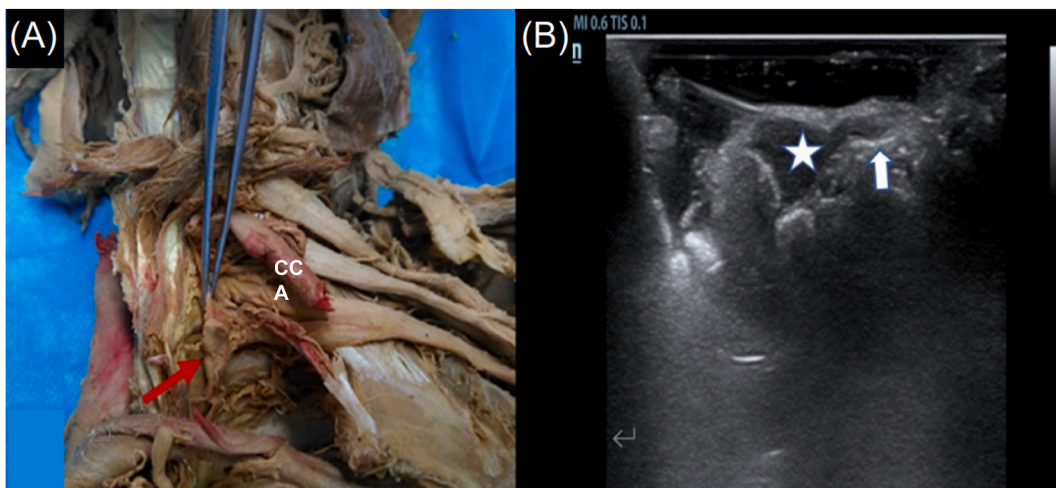


Fig. 1. Specimen of cervical sympathetic chain and corresponding ultrasound image. (A) Red arrow shows the ganglion and the ribbon-like structure held by the forceps is sympathetic nerve. (B) White star shows the oval ganglion and white arrow shows the connected nerve. CCA, Common carotid artery. (For interpretation of the references to colour in this figure legend, the reader is referred to the Web version of this article.)

The ultrasonographic examination of the left side of the neck in male Y revealed a hypoechoic nodule in continuity with the cervical sympathetic chain. Subsequently, we identified a hypoechoic nodule that was not connected to the nerves, with a hilum-like structure in the center, as is shown in Fig. 2. We assumed that this structure was a lymph node, which was also dissected and pathologically examined. No obvious mCSG-like structures were detected on the right side of the neck in male Y. In male O, suspected CSG hypoechoic nodules were detected on both sides, and a core-needle biopsy was performed on both.

Regarding the samples submitted for pathological examination, two histopathologists examined the sections and provided consistent histological identifications: Fig. 3A,B is the histological section of specimen 1 of cadaveric male Y's neck, exhibiting typical lymph node structure, consistent with the ultrasonographic evaluation, whereas specimens 2, 3, and 4 were sympathetic ganglion tissues (Fig. 4), also consistent with the ultrasonographic evaluation.

3. Discussion

Minimally invasive US-guided procedures in the neck have become more common in recent years, including CSG block, the radiofrequency ablation of thyroid or parathyroid nodules, and the biopsies of neck masses. These procedures bear the risk of intermittent or permanent CSG damage [7,14]. Hence, understanding the sono-anatomical and imaging characteristics of the mCSG is crucial. High-frequency transducer imaging technology is a promising technique for the direct visualization of the mCSG.

Apart from anatomical research, literature on the mCSG is limited, particularly US-based studies. The mCSG has been previously identified on US imaging as an oval hypoechoic structure with at least two connected hypoechoic linear structures; the latter appear as multi-nerve fibers connected to the mCSG. However, to the best of our knowledge, no previous study has confirmed these sonographic features either anatomically or pathologically as in the present study [15]. Peripheral nerves, such as the sciatic or ulnar nerve, are known to appear on US images as multiple hypoechoic parallel linear structures separated by hyperechoic bands, corresponding to the longitudinal neuronal fascicles within the nerves. In contrast, the cervical sympathetic trunk assumes an elongated, thin hypoechoic appearance on US images, possibly because its internal components are below the resolution threshold of US imaging.

The most accepted injection positions for SGB are the anterior tubercle of the C6 transverse process and the level of C7, and the probabilities of stellate ganglia staining are 45 % and 63 %, respectively [16,17]. A possible reason for this finding may be anatomical variations in the CSG position. Shin et al. [13] found that the mCSG occasionally lies medially to the common carotid artery, distant from the tubercle. Previous studies have suggested that the mCSG may be adjacent to the posterior wall of the carotid sheath [12,13]. All these variations in the mCSG position potentially contribute to the SGB variable efficacy. Therefore, a sono-anatomical study of the mCSG may assist in the preoperative identification and localization of the mCSG and cervical sympathetic trunk, thereby increasing the accuracy of SGB. Using US imaging to position the needle accurately near the mCSG may help minimize the dose of local anesthetic required and reduce the incidence of complications, thus improving the safety and efficacy of the procedure.

The mCSG is prone to damage during the US-guided biopsy or radiofrequency ablation of thyroid and parathyroid tumors due to its anatomical proximity to these glands. Therefore, monitoring the mCSG with US imaging is valuable during these procedures. The injection of 5 % dextrose in water between the thyroid tumor and mCSG potentially prevents thermal damage to the latter during the ablation procedure.

Since the mCSG are predominantly assumed to be in a typical location, the main purpose of investigating their actual position is to protect them from iatrogenic damage. However, anatomical confirmation in this study was performed on cadaveric specimens and fresh cadavers to clarify the imaging features of the mCSG, and in these samples they may differ slightly from those in vivo. Therefore, further confirmation in vivo is warranted. Verification bias was controlled using strict criteria based on the literature review. In addition, Lee et al. [11] suggested that intraganglionic hypointensity, which possibly reflects a vessel or fatty connective tissue, could indicate the position of the CSG. Therefore, further contrast-enhanced US imaging may be required to explore the blood supply of the mCSG and cervical sympathetic trunk.

Our research still had some limitations. First, we only verified the location and ultrasound features of the mCSG on cadavers and specimens. The next step is to validate our ultrasound findings on healthy individuals. Second, due to the widespread use of ultrasound-guided SGB in clinical practice, further large-scale comparative studies can be conducted to see whether the visualization of mCSG by HRUS can improve the SGB efficacy and reduce accidental injury to adjacent structures.

In conclusion, the direct visualization of the mCSG using HRUS is feasible, based on an adequate understanding of both its location and imaging features. This knowledge may reduce the incidence of surgical complications and improve the accuracy of US-guided neck interventional procedures.

Table 1
Cadaveric sampling results.

Cadaver	Neck side	Ultrasound finding	Sample number	Anatomy	Pathology
Male Y	Left	One suspected lymph node	No. 1	Confirmed	Lymph node
		One suspected CSG	No. 2	Confirmed	Nerve tissue
Male O	Right	None	–	–	–
	Left	One suspected CSG	No. 3	Confirmed	Nerve tissue
		One suspected CSG	No. 4	Confirmed	Nerve tissue

CSG: cervical sympathetic ganglion; No.: number; -: absent.

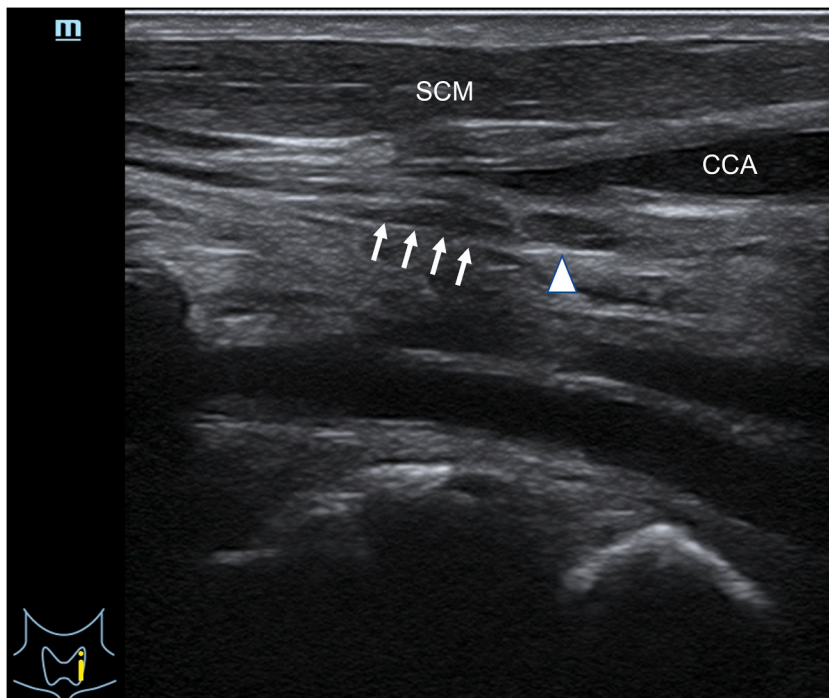


Fig. 2. Ultrasound image of Male Y's mCSG and lymph node in left neck. White arrow shows the mCSG, white arrow head shows the adjacent lymph node. SCM, Sternocleidomastoid muscle; CCA, Common carotid artery.

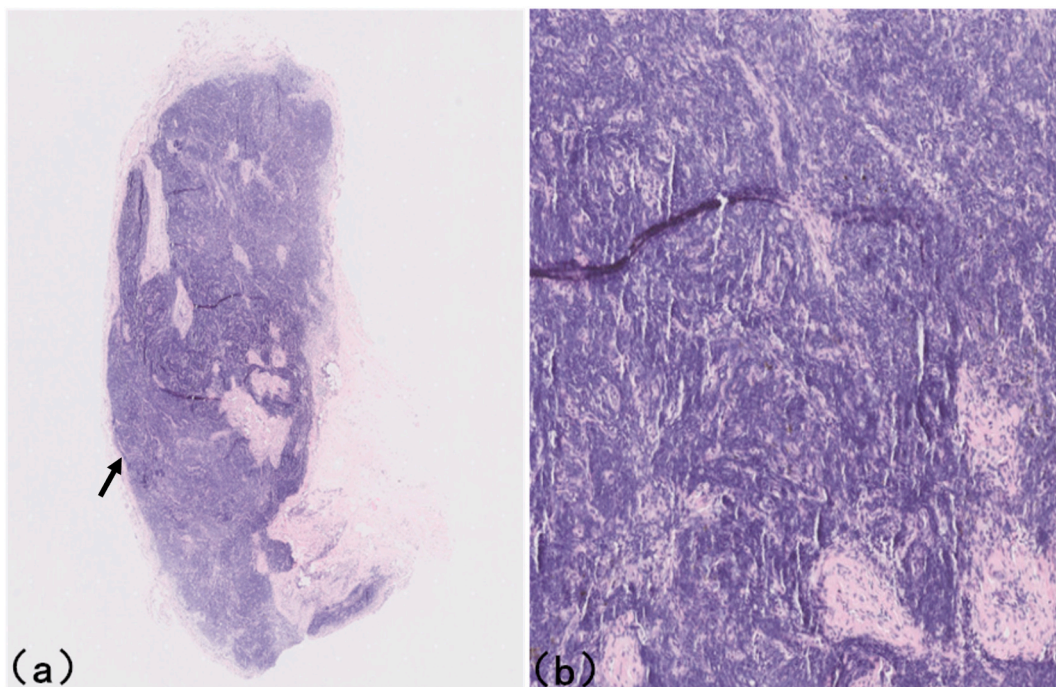


Fig. 3. Histological section of specimen 1 of cadaveric male Y's neck, exhibiting typical lymph node structure. (a) haematoxylin-eosin stain, original magnification, Black arrow shows the lymphoid follicle; (B) haematoxylin-eosin stain, original magnification $\times 6$.

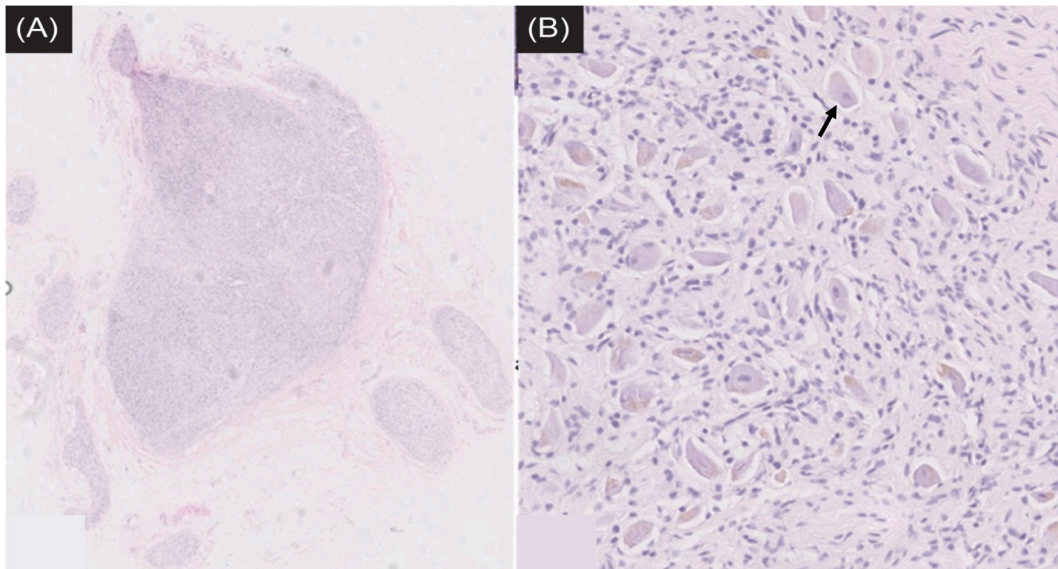


Fig. 4. Histological section of specimen 2 of cadaveric male Y's neck, confirmed to be a ganglion.(A) haematoxylin-eosin stain, original magnification. (B) haematoxylin-eosin stain, original magnification $\times 8$, Black arrow shows the ganglion cell.

4. Materials and methods

4.1. Study specimens

The study was conducted in accordance with the Declaration of Helsinki and approved by the Institutional Review Board of Peking University Third Hospital (approval number: M2017318, issued date: November 21, 2017). The requirement for informed consent was waived for this cadaveric study. The authors hereby confirm that every effort was made to comply with all local and international ethical guidelines and laws concerning the use of human cadaveric donors in anatomical research.

The study was conducted on three dissected teaching specimens and two frozen male cadavers. The sex and age of the teaching specimens were unknown. In the three teaching specimens, the cervical sympathetic trunk was dissected clearly and completely; however, it remained in the neck-shoulder region. The necks of the cadavers were well preserved, and the cervical skin was free of

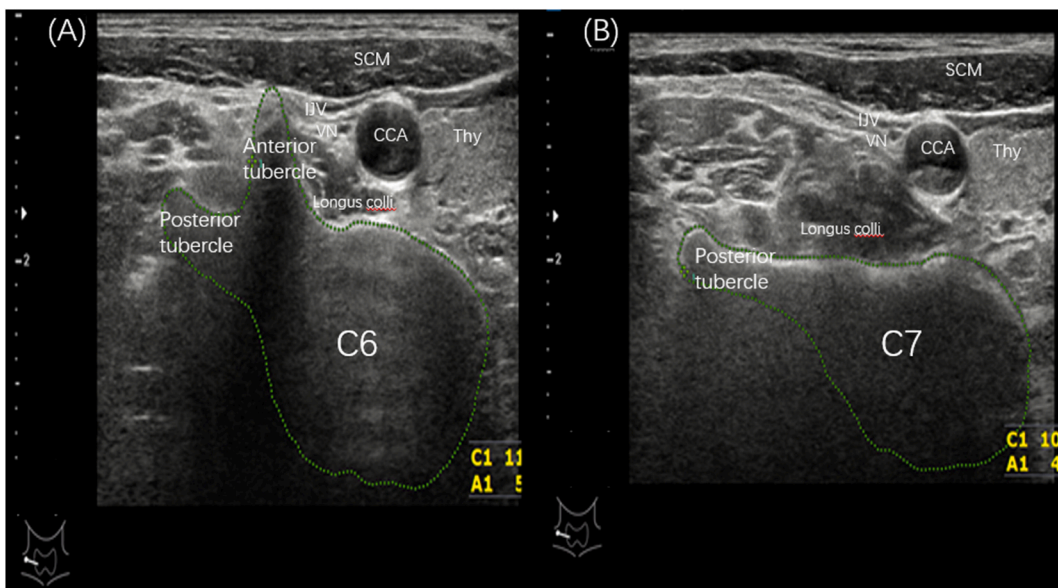


Fig. 5. (A) shows the sonogram of C6 with anterior tubercle and posterior tubercle, (B) shows the sonogram of C7 with only posterior tubercle. SCM, Sternocleidomastoid muscle; IJV, Internal jugular vein; VN, Vagus nerve; CCA, Common carotid artery; Thy, Thyroid.

trauma and surgical scarring. The cadavers were named male Y and male O.

4.2. Ultrasonographic and anatomical examination of the specimens and cadavers

First, the direct HRUS scanning of the CSG was performed on the three head and neck specimens, with the cervical sympathetic trunk integrally dissected and coated with a substantial coupling agent quantity. The images were digitally recorded on the hard drive of the US scanning unit.

Then, the HRUS scanning of the neck was performed bilaterally on the two cadavers. The mCSG was identified based on descriptions of its anatomical position from previous studies with cadaveric dissection and the HRUS images acquired during the direct specimen scanning. The mCSG of the first cadaver was localized using a breast localization wire and single-use introducer needle (SOMATEX Medical Technologies GmbH, Berlin, Germany); subsequently, it was dissected by an anatomical technician with more than 20 years of experience in anatomy to verify whether the structure identified was indeed the mCSG. US-guided core-needle biopsy was performed in the second cadaver on the suspected mCSG. All tissues were stained with haematoxylin-eosin at the Peking University Third Hospital Central Laboratory to confirm their anatomical identification via pathological examination.

All sonographic examinations were performed using devices by Mindray M9 (Mindray, Shenzhen, China), equipped with high-frequency linear probes (5–14 MHz) in the “Thyroid Scan” mode.

4.3. Ultrasonographic scanning of the mCSG

First, the transverse processes of C6 and C7 were identified through continually scanning one side of the neck, with the probe placed in a transverse orientation. The identification was based on the presence of an anterior and posterior transverse tubercle on the C6 transverse process (Fig. 5A), whereas 98 % of C7 vertebrae only possess a posterior transverse tubercle on the transverse process [18] (Fig. 5B). After the localization of the cervical segment, US scanning was performed between C5 and C7. A hypoechoic bulbous node lying superficially on the cervical longus muscle, posterior to the carotid sheath, and surrounding other anatomical structures, such as the thyroid gland and inferior thyroid artery, was subsequently sought. The sonographic appearance of the CSG is characterized by ovoid hypoechoic nodules connected to multiple linear hypoechoic lines with clear boundaries, a homogeneous echo signal, and no hilar structure, typical of the lymph nodes. Once we identified a suspected mCSG, the scanner was rotated longitudinally to determine whether the suspected ganglion had at least two thin, linear hypoechoic structures running parallel in the cephalad and caudad directions, suggesting the anatomy of the sympathetic trunk.

4.4. Puncture sampling process

US-guided specimen sampling was performed on the hypoechoic nodules conforming to the CSG characteristics. The position of the neck was fixed during the scanning. Generally, the probe had to form an angle of 30–40° with the sagittal plane of the neck. The puncture needle was inserted outside of the ultrasonic probe (in-plane technology) and placed in the ultrasonic scanning plane, showing a strong linear echo on the sonographic screen. The needle route simulated the CSG block route in vivo. During the puncture procedure, the needle could be inserted and withdrawn within a small range to determine the most appropriate entry route and needle-tip position. After the targeted CSG was successfully punctured in one of the specimens, the hollow cannula was removed, while the solid needle core remained in the nodule, which was subsequently dissected along the layers of the needle core; finally, the nodule was fixed by removing the positioning needle. The remaining specimen was sampled using a biopsy needle. The nodules were sampled using an 18-G puncture needle under US guidance. Fig. 6(A–D) shows the sampling process for the mCSG. The specimens were then stored in formaldehyde bottles. Each nodule was effectively sampled at least three times to ensure that the tissue was sufficient. During the process of needle placement and puncture, dynamic and static images were recorded for analysis.

4.5. Pathology

Pathologic samples were stained with haematoxylin and eosin at the Peking University Third Hospital Central Laboratory by two pathologists with 10 years of experience to confirm whether the anatomical identification was correct.

Additional information

No additional information is available for this paper.

Funding

This research did not receive any specific grant from funding agencies in the public, commercial, or not-for-profit sectors.

Data availability statement

The datasets used and/or analyzed during the current study are available from the corresponding author on reasonable request.

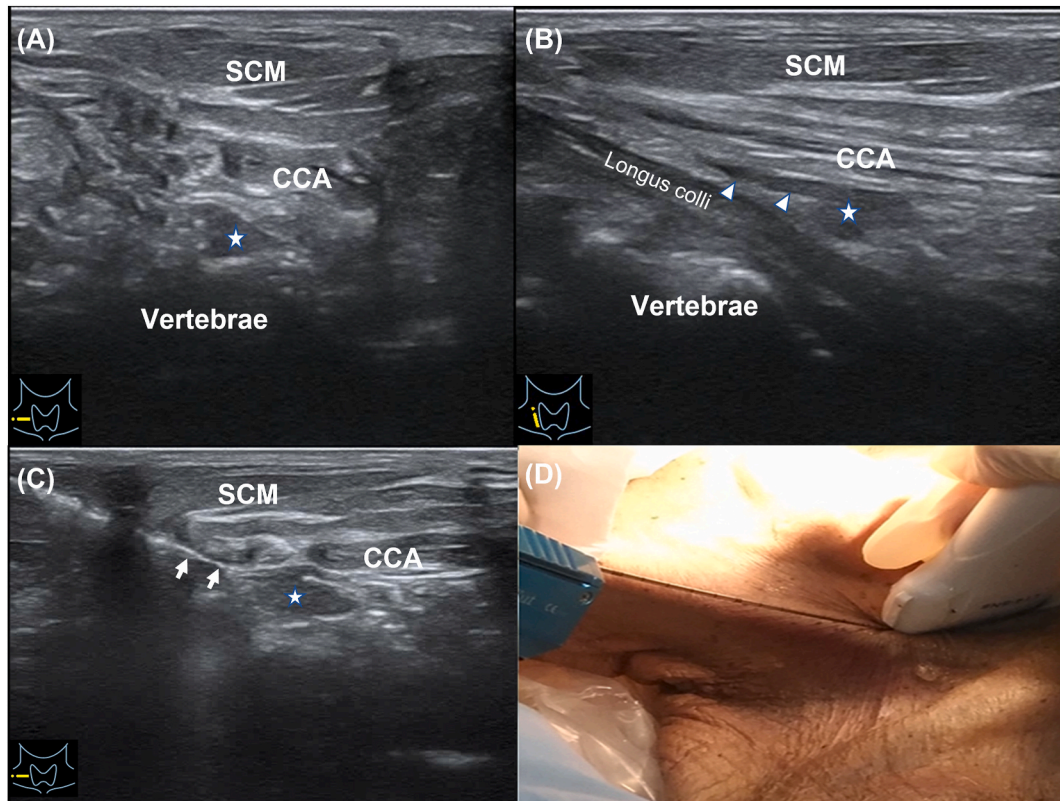


Fig. 6. Sampling process for the mCSG. (A) shows the transverse sonogram of mCSG, white star is the mCSG. (B) shows the long-axis ultrasound image of mCSG, white arrow head is the connected sympathetic nerve chain. (C) shows the biopsy of mCSG, white arrow is the puncture needle. (D) is the according picture of the process of biopsy. CCA, Common carotid artery; SCM, Sternocleidomastoid muscle.

CRedit authorship contribution statement

Yu-Tao Lei: Investigation, Methodology, Project administration. **Yun-Xia Hao:** Methodology, Project administration, Writing – original draft. **Zhen Yang:** Project administration, Writing – original draft. **Zhuo-Hua Lin:** Project administration. **Wen Qin:** Investigation. **Jun-Hao Yan:** Project administration. **Yang Sun:** Project administration. **Li-Gang Cui:** Investigation, Methodology, Project administration, Supervision, Writing – review & editing. **Ying Fu:** Project administration, Writing – review & editing.

Declaration of competing interest

The authors declare that they have no known competing financial interests or personal relationships that could have appeared to influence the work reported in this paper.

Acknowledgments

None.

References

- [1] E.L. Malmqvist, M. Bengtsson, J. Sörensen, Efficacy of stellate ganglion block: a clinical study with bupivacaine, *Reg. Anesth.* 17 (6) (1992) 340–347.
- [2] E. Piraccini, S. Munakomi, K.V. Chang, Stellate ganglion blocks, in: StatPearls. Treasure Island (FL), StatPearls Publishing, 2023. August 13.
- [3] S. Narouze, Ultrasound-guided stellate ganglion block: safety and efficacy, *Curr. Pain Headache Rep.* 18 (6) (2014) 424.
- [4] S. Kapral, P. Krafft, M. Gosch, D. Fleischmann, C. Weinstabl, Ultrasound imaging for stellate ganglion block: direct visualization of puncture site and local anesthetic spread. A pilot study, *Reg. Anesth.* 20 (4) (1995) 323–328.
- [5] A. Kastler, S. Aubry, N. Saille, et al., CT-guided stellate ganglion blockade vs. radiofrequency neurolysis in the management of refractory type I complex regional pain syndrome of the upper limb, *Eur. Radiol.* 23 (5) (2013) 1316–1322.
- [6] E.J. Ha, J.H. Baek, J.H. Lee, Ultrasonography-based thyroidal and Perithyroidal anatomy and its clinical significance, *Korean J. Radiol.* 16 (4) (2015 Jul-Aug) 749–766.
- [7] D.G. Na, J.H. Lee, S.L. Jung, et al., Radiofrequency ablation of benign thyroid nodules and recurrent thyroid cancers: consensus statement and recommendations, *Korean J. Radiol.* 13 (2) (2012) 117–125.

- [8] G.R. Pishdad, P. Pishdad, R. Pishdad, Horner's syndrome as a complication of percutaneous ethanol treatment of thyroid nodule, *Thyroid* 21 (3) (2011) 327–328.
- [9] J.E. Shin, J.H. Baek, J.H. Lee, Radiofrequency and ethanol ablation for the treatment of recurrent thyroid cancers: current status and challenges, *Curr. Opin. Oncol.* 25 (1) (2013) 14–19.
- [10] F. Lu, J. Tian, J. Dong, K. Zhang, Tonic-clonic seizure during the ultrasound-guided stellate ganglion block because of an injection into an unrecognized variant vertebral artery: a case report, *Medicine (Baltim.)* 98 (48) (2019) e18168.
- [11] J.Y. Lee, J.H. Lee, J.S. Song, M.J. Song, S.J. Hwang, R.G. Yoon, S.W. Jang, J.E. Park, Y.J. Heo, Y.J. Choi, J.H. Baek, Superior cervical sympathetic ganglion: normal imaging appearance on 3T-MRI, *Korean J. Radiol.* 17 (5) (2016 Sep-Oct) 657–663.
- [12] A. Chaudhry, A. Kamali, D.A. Herzka, K.C. Wang, J.A. Carrino, A.M. Blitz, Detection of the stellate and thoracic sympathetic chain ganglia with high-resolution 3D-CISS MR imaging, *AJNR Am J Neuroradiol* 39 (8) (2018) 1550–1554.
- [13] J.E. Shin, J.H. Baek, E.J. Ha, Y.J. Choi, W.J. Choi, J.H. Lee, Ultrasound features of middle cervical sympathetic ganglion, *Clin. J. Pain* 31 (10) (2015) 909–913.
- [14] O. Messika, G. Telman, Horner syndrome after lymph node fine needle aspiration, *Acta Cytol.* 53 (4) (2009) 487–488.
- [15] J. Li, S. Pu, Z. Liu, L. Jiang, Y. Zheng, Visualizing stellate ganglion with US imaging for guided SGB treatment: a feasibility study with healthy adults, *Front. Neurosci.* 16 (2022) 998937.
- [16] G.C. Feigl, W. Rosmarin, A. Stelzl, B. Weninger, R. Likar, Comparison of different injectate volumes for stellate ganglion block: an anatomic and radiologic study, *Reg. Anesth. Pain Med.* 32 (3) (2007) 203–208.
- [17] C. Park, C.H. Suh, J.E. Shin, J.H. Baek, Characteristics of the middle cervical sympathetic ganglion: a systematic review and meta-analysis, *Pain Physician* 21 (1) (2018) 9–18.
- [18] P. Soeding, N. Eizenberg, Review article: anatomical considerations for ultrasound guidance for regional anesthesia of the neck and upper limb, *Can. J. Anaesth.* 56 (7) (2009) 518–533.